

NBSIR 75-957

Finite Element Analysis of Spotwelded, Bonded and Weldbonded Lap Joints

Richard A. Mitchell, Ruth M. Woolley, and Saul M. Baker

Engineering Mechanics Section
Mechanics Division
Institute for Basic Standards
National Bureau of Standards
Washington, D. C. 20234

December 1975

Final

19960319 141

Prepared for
National Bureau of Standards
Washington, D. C. 20234

DISTRIBUTION STATEMENT A

Approved for public release
Distribution Unlimited

PLASTICS TECHNICAL EVALUATION CENTER
PICATINNY ARSENAL, DOWRY, N. J.

DTIC QUALITY INSPECTED 1

PLASTIC 23855

75042156

NBSIR 75-957

**FINITE ELEMENT ANALYSIS OF
SPOTWELDED, BONDED AND
WELDBONDED LAP JOINTS**

Richard A. Mitchell, Ruth M. Woolley, and Saul M. Baker

Engineering Mechanics Section
Mechanics Division
Institute for Basic Standards
National Bureau of Standards
Washington, D. C. 20234

December 1975

Final

Prepared for
National Bureau of Standards
Washington, D. C. 20234



U.S. DEPARTMENT OF COMMERCE, Elliot L. Richardson, *Secretary*
James A. Baker, III, *Under Secretary*
Dr. Betsy Ancker-Johnson, *Assistant Secretary for Science and Technology*
NATIONAL BUREAU OF STANDARDS, Ernest Ambler, *Acting Director*

FINITE ELEMENT ANALYSIS OF SPOTWELDED, BONDED AND WELDBONDED LAP JOINTS

Richard A. Mitchell, Ruth M. Woolley, and Saul M. Baker

ABSTRACT

[Finite element computer analyses of single-lap and double-lap structural joints are described. A planform analysis articulates the in-plane deformation of the joined sheet material and the lap-shear stresses acting through the spotwelds and/or adhesive. A longitudinal cross-section analysis computes out-of-plane bending effects, particularly important in single-lap joints, and adhesive peel stresses.] Numerical results are presented that suggest a reasonable degree of mutual consistency between the planform analysis and the cross-section analysis. Although the basic finite element formulation is linear, nonlinear deformation can be simulated by a series of linear solutions. [The computer output includes contour plots of stress and strain fields and exaggerated-scale plots of displacements.]

Key Words: Adhesive-bonded joints; bonded joints; double-lap-joint analysis; finite element analysis; joining; joints; single-lap-joint analysis; single-lap-joint bending; spotwelded joints; weldbonded joints.

1. INTRODUCTION

Both spotwelding and adhesive bonding are well established methods for joining metal sheet. Weldbonding, a comparatively new joining method that combines both spotwelding and adhesive bonding in the same joint, offers several potential advantages over either method alone (see, for example, Ref. 1-4). In some cases a weldbonded joint can be fabricated for less cost than a bonded joint because the spotwelds hold the joint together during the curing process. Under some loading and environmental conditions the spotwelds can function as "crack arresters" in retarding the growth of a progressive debond within the adhesive. The spotwelds also can give a weldbonded joint greater peel strength than a comparable bonded joint. The adhesive component gives a weldbonded joint greater static, impact, and fatigue strength; greater stiffness (less shear lag); greater damping capacity; and greater durability than a comparable spotwelded joint. The adhesive component also functions as a seal against the passage of gas, liquid, or dust.

Finite element analysis is particularly suitable for the study of these joints because of their geometric complexity and because of the great differences in the mechanical properties of the interacting materials. An important application of the analysis is in the quantitative interpretation of laboratory tensile-shear tests of lap joint specimens. Critical values of stress and strain cannot be estimated directly from these laboratory measurements without some understanding of the highly nonuniform stress and strain fields in the interior of the joint. Beyond this application, the analysis can be used in studying general performance characteristics of these joints and in optimizing their design.

Separate finite element computer programs were developed for the planform analysis and the longitudinal cross-section analysis of a broad class of spotwelded, bonded, and weldbonded single-lap and double-lap joint configurations. The joint materials can be either isotropic or orthotropic, as defined by four independent elastic constants. Although the basic finite element formulation is linear, the analytical approach permits nonlinear deformation and progressive debonding to be approximated by a series of linear solutions. In an extension of the work reported here, the computer programs are being used to study the response of weldbonded joints loaded well into the nonlinear range of the adhesive*.

The analyses described here could also be applied to other material combinations and joining processes. Some examples are: (1) weldbrazed joints of metal or metal-matrix composite [5]; (2) spotwelded or weldbonded joints of metal-matrix composite [6]; and (3) bonded joints of composite [7-10]. A variation of the analysis could be used to study joints formed by a combination of adhesive bonding and either riveting or bolting [7,8]. For the analysis of such joints, however, the effective shear stiffness of the fastener mechanisms must be estimated, analytically and/or empirically, taking into account such complications as fastener slip, fastener bending, inelastic bearing deformation, and interference fit.

2. WELDBOND CONFIGURATION

Figure 1 is a schematic (not to scale) detail of a spotweld and the surrounding adhesive-bonded region of a single-lap weldbonded joint. In perhaps the most commonly used weldbonding process, a paste adhesive is applied to the metal sheet material, and then the metal is spotwelded through the uncured adhesive. The spotwelding pressure and heat result in displacement of the adhesive and fusion of the metal to form a solid weld nugget. In Figure 1, the solid circle represents the visible mark at the edge of the surface of contact between the spotwelding electrode and the metal sheet. The inner dashed circle outlines the weld nugget. The area between the two dashed circles, sometimes referred to as a "halo", is effectively unbonded due to the displacement and heating

*This analytical study of nonlinear response and a parallel experimental study, both sponsored by Feltman Research Laboratory, Picatinny Arsenal, Dover, N. J., will be the subject of a later report.

of the adhesive during the spotwelding process. Beyond the halo is a region of transition to full adhesive thickness. The precise shape and dimensions of these spotweld features are functions of several variables, including the thickness and stiffness of both the metal sheet and the uncured adhesive and such welding parameters as pressure, current, resistance, time, and electrode shape.

Figure 2 shows a single-lap welded joint and a comparable double-lap joint. These joint configurations are discussed below in numerical examples.

3. PLANFORM ANALYSIS

The general approach used here parallels one used earlier for the planform analysis of composite-reinforced cutouts and cracks [9,10]. Figure 3(a) shows the network of triangular finite elements used for the analysis of the welded joint shown in Figure 2 and a similar spotwelded joint. Figure 3(b) shows the network used for the analysis of a similar bonded joint. Because of symmetry about the x axis, only the upper half of a joint is analyzed. The joined sheets are each divided into separate networks of triangular, constant strain (linearly varying displacement), plane stress elements that are congruent within the overlap region. Within a bonded and/or welded region the two congruent networks are coupled together by an array of special shear-stiffness elements linking conjugate pairs of nodal points. External normal and shear loads are assumed to act only at the edge and in the midplane of a sheet, and out-of-plane deflections are ignored. The direct stiffness matrices of the triangular elements are computed in the usual way (see, for example, Zienkiewicz [11]). A different formulation is required for computation of the shear-stiffness coupling elements, however.

Figures 4(a) and 4(b) show, respectively, schematic plan and cross-section views of part of the adhesive-bonded region of a lap joint. In Figure 4(b) the x axis is a free boundary in the case of a single-lap joint; it is a line of symmetry in the case of a double-lap joint. Within the area of a spotweld nugget (Fig. 1) there is no adhesive and the two metal sheets are assumed to be perfectly joined (continuous). There is also no adhesive in the halo region surrounding a nugget but here the two metal sheets are assumed to be unbonded. Within the shear-stiffness element the shear stress is assumed to vary linearly through the metal sheet thickness as shown in Figure 4(c). That is, the shear stress is assumed to have a maximum value at the adhesive layer (c to d), or at the midplane of a weld nugget, and to decrease uniformly to zero at a free surface (a or f) or at a plane of symmetry (a). The effective area of a shear-stiffness element in the x-y plane is assumed to be equal to one-third the sum of the triangular areas meeting at an overlap nodal point. The effective material thicknesses within an element are assumed to be the thicknesses at the location of the conjugate nodal points.

The nodal point stiffness matrix for a shear-stiffness element relates the components of shear force acting in the adhesive layer or

weld nugget to the components of relative displacement of the joined sheets by the expression

$$\begin{Bmatrix} f_{sx} \\ f_{sy} \end{Bmatrix} = \begin{bmatrix} k_{sx} & 0 \\ 0 & k_{sy} \end{bmatrix} \begin{Bmatrix} u_s \\ v_s \end{Bmatrix} \quad (1)$$

in which u_s and v_s are, respectively, the x and y components of the difference^s in displacement of the midplanes of the sheets. By assuming that each shear-stiffness element is deformed in pure shear, the relative displacement within the element can be approximated by an integral of the form

$$u_{s\ me} = \int_m^c \frac{\tau_{xz}}{G_1} dz + \int_c^d \frac{\tau_{xz}}{G_2} dz + \int_d^e \frac{\tau_{xz}}{G_3} dz \quad (2)$$

in which

$m = a$ in the case of a double-lap joint,

$m = b$ in the case of a single-lap joint,

$(u_{s\ me})$ = difference between x components of displacement at points e and m (point a or b in Fig. 4(b)),

and G_1 , G_2 , and G_3 are, respectively, the shear moduli of the lower sheet, the adhesive, and the upper sheet. In the double-lap joint case, integration of eq. (2) between points a and e and substitution into eq. (1) gives the shear-stiffness coefficient

$$k_{sx} = \frac{A_s}{\frac{1}{2} \frac{t_1}{G_1} + \frac{t_2}{G_2} + \frac{3}{8} \frac{t_3}{G_3}} = k_{sy} \quad (3)$$

in which

A_s = the area of the shear-stiffness element in the x-y plane,

t_1 = one-half the thickness of the lower (inner) sheet of the double-lap joint,

t_2 = the thickness of the adhesive, or zero within a nugget area,

t_3 = the thickness of upper (outer) sheet of the double-lap joint.

In the single-lap joint case, integration of eq. (2) between points b and e (Fig. 4(b)) and substitution into eq. (1) gives the shear-stiffness coefficient

$$\bar{k}_{sx} = \frac{A_s}{\frac{3}{8} \frac{t_1}{G_1} + \frac{t_2}{G_2} + \frac{3}{8} \frac{t_3}{G_3}} = \bar{k}_{sy} \quad (4)$$

in which t_1 and t_3 are, respectively, the thickness of the lower and upper sheet, and the other symbols are defined as above.

The stiffness matrices of the triangular and the shear-stiffness elements are superposed to form the stiffness matrix of the entire structure. This latter matrix $[K]$ relates the external forces applied to the joint $\{F\}$ to the resulting nodal point displacements $\{w\}$ according to the equation

$$\{F\} = [K] \{w\} \quad (5)$$

This equation can be solved for nodal point displacements $\{w\}$ throughout the joint. Then, strains and stresses within the triangular elements can be computed in the usual way [11]. The lap shear stresses $\{\tau\}$ are obtained by dividing the lap shear forces $\{f_s\}$ by the shear area A_s ; that is

$$\begin{Bmatrix} \tau_{sx} \\ \tau_{sy} \end{Bmatrix} = \frac{1}{A_s} \begin{bmatrix} k_{sx} & 0 \\ 0 & k_{sy} \end{bmatrix} \begin{Bmatrix} u_s \\ v_s \end{Bmatrix} \quad (6)$$

The lap shear stress components τ_{sx} and τ_{sy} can be added vectorially to give the resultant lap shear stress τ_s at each nodal point within the bonded, welded, or weldbonded area.

The stress contour plots in Figures 5 and 6 provide examples of the results of this analysis for single-lap spotwelded, bonded, and weldbonded joints similar to the one shown in Figure 2, using the finite element networks shown in Figure 3. For these solutions the left boundary was constrained with respect to x displacement and the right boundary was subjected to a uniform tensile stress of 10,000 lbf/in² (68.95×10^6 Pa). The joint materials were assumed to be linear elastic and isotropic with the following elastic constants:

Metal sheet: $E = 9.92 \times 10^6$ lbf/in² (68.4×10^9 Pa)

$\nu = 0.318$

Adhesive: $E = 0.677 \times 10^6 \text{ lbf/in}^2 (4.67 \times 10^9 \text{ Pa})$

$\nu = 0.35$

The mesh pattern of zero-value lap shear stress contours in Figures 5(a) and 5(c) indicate, respectively, the unbonded region of the spotwelded joint and the unbonded halo region around the weldbond nuggets. The peak-value lap shear stress contour at the spotweld in Figure 5(a) is $16,000 \text{ lbf/in}^2 (110.3 \times 10^6 \text{ Pa})$. The peak-value tensile stress contour at the rightmost spotweld in Figure 6(a) is $15,000 \text{ lbf/in}^2 (103.4 \times 10^6 \text{ Pa})$.

4. LONGITUDINAL CROSS-SECTION ANALYSIS

Figure 7 shows finite element networks used for the cross-section analysis of the comparable single-lap and double-lap weldbonded joints described in Figure 2, subjected to a tensile stress of $10,000 \text{ lbf/in}^2 (68.95 \times 10^6 \text{ Pa})$. Thickness dimensions are exaggerated 4 times, and computed vertical deflections are exaggerated 20 times. In the doublelap case, symmetry is imposed about the horizontal (x) axis. In the cross-section analysis, linearly varying strain (quadratically varying displacement) elements are used to better approximate out-of-plane bending. The direct stiffness matrices of the triangular elements are computed using the area coordinate formulation described by Zienkiewicz [11]. The spotweld nuggets are approximated by triangular bond-line elements of metal, rather than adhesive, equal in area (in-plan) to the circular area of the spotwelds. A nugget region is bounded on each side by a region of transition to full adhesive thickness. The bondline thickness in a nugget or transition region is reduced to approximate the average adhesive thickness.

Figure 8 shows contour plots of the computed longitudinal normal stress in the single-lap weldbonded joint and the comparable double-lap joint. In each case the sheet mid-thickness point at the left end (Fig. 7) was constrained with respect to x displacement and the load was applied to the mid-thickness point (of the finite element network) at the right end. The high stress gradients indicated by the dark regions at the ends of each contour plot are only local effects due to concentrating the boundary loading at single points. Note the high tensile stresses and stress gradients in the metal sheet of the single-lap joint, adjacent to the adhesive, at each end of the overlap. The strains associated with these stresses are probably a major factor in the initiation of adhesive bond failure in these joints. The comparable double-lap joint has significantly smaller tensile stresses and stress gradients in these regions.

5. COMPARISON OF NUMERICAL RESULTS

Figure 9 compares the adhesive shear stresses for the single-lap weldbonded joint (Fig. 2) as computed by the planform analysis with those computed by the cross-section analysis. The difference in shear stress distribution is largely due to joint bending which is included

in the cross-section analysis but not in the planform analysis. This explanation is supported by a similar plot for a comparable double-lap joint (Fig. 10) which shows much better agreement between the planform and the cross-section analyses.

Figure 11 compares the adhesive normal stresses (peel component, σ_z) computed by the cross-section analysis for both the single-lap and comparable double-lap welded joints. The peak tensile stress values at the right end differ by less than 6 percent. The symmetry constraint imposed in the double-lap case causes the normal stress peak to be compressive at the left end. Peel stresses are not computed in the planform analysis.

Figure 12 compares the strains on the upper surface of the single-lap welded joint (Fig. 2) as computed by the planform analysis with those computed by the cross-section analysis. The plotted points were obtained by applying a bending correction to the planform results. The bending curvatures (evident in Fig. 7) were determined from the cross-section results by fitting a second degree curve through groups of five adjacent nodal points along the length of the joint. The components of surface strain due to bending were then computed directly from these curvatures by assuming a linear variation in bending strain through the joint thickness.

Figures 7(a), 9, and 12 illustrate some dominant characteristics of single lap joints of these proportions. When these joints are loaded in tension, bending moments of like sign develop just inside each end of the overlap region, and transverse shear forces of opposite sign form a moment couple to balance the bending moments. Thus, there is a uniform transverse shear force resultant and a linearly varying bending moment acting in the interior of the overlap region. This explains the approximately uniform shear stress (Fig. 9) and linearly varying bending strain (Fig. 12) evident over most of the overlap length. There is a reversal in bending direction just inside each end and at midlength of the overlap region (Fig. 7(a)).

Figure 13 compares the surface strains for the double-lap welded joint (Fig. 2) as computed by the planform analysis with those computed by the cross-section analysis. Although bending is prevented by symmetry along the x axis in the cross-section analysis, there is some bending of the outer sheet at each end of the overlap, and there is considerable bending beyond the overlap (Fig. 7). The plotted points were obtained by applying a bending correction (from the cross-section analysis) to the planform results.

Successive overrelaxation, along with group relaxation [12], was used to obtain these numerical results. Each planform solution required less than one hundred cycles of iteration. The relatively good shape, uniformity, and spacial distribution of the triangular planform elements contributed to this computational efficiency. The cross-section solutions for double-lap joints were slower to converge, probably due to

the poor shape of the adhesive elements, the long spacial distribution of the network, and the great differences in material stiffnesses. The cross-section solutions for single-lap joints were the slowest to converge, due to the large bending displacements. Marginally converged solutions required as much as a thousand cycles of iteration, in some cases involving multiple computer runs in order to subjectively adjust the overrelaxation and group relaxation parameters.

6. CONCLUSION

Both the planform analysis and the cross-section analysis should be useful in the study of bonded and weldbonded lap joints. The planform analysis should also be useful in the study of spotwelded joints, but the cross-section analysis is not recommended for these joints because of the complications of biaxial bending and relative transverse displacement in the unbonded overlap regions. The planform analysis alone may be adequate for most purposes in the study of either double-lap joints or single-lap joints that are constrained to prevent excessive bending. Where out-of-plane bending or peel stresses are important, however, in either bonded or weldbonded joints, the planform analysis should be supplemented by the cross-section analysis.

7. REFERENCES

1. Semerdjiev, S., Metal-to-Metal Adhesive Bonding, Business Books (1970).
2. Kizer, J. A., and Grosko, J. J., Development of the Weldbond Joining Process for Aircraft Structures, Proc. Symp. on Processing for Adhesive Bonded Structures, Stevens Inst. Tech. (Aug. 1972).
3. Mahon, J., Vizzi, C., Sisco, W., and Nilsson, P., Aluminum Weld-bonding for 350 °F Service, Proc. 5th Nat. SAMPE Tech. Conf. (Oct. 1973).
4. Tenerelli, D. J. and Houghey, V. A., Improved Approach to Structural Integrity of Spacecraft Shrouds by Use of Skin-Corrugated Weldbond (Spotweld/Adhesive Bond), AIAA Paper No. 74-381 (Apr. 1974).
5. Bales, T. T., Royster, D. M., and Arnold, W. E., Jr., Weld-Brazing of Titanium, Proc. 5th Nat. SAMPE Tech. Conf. (Oct. 1973).
6. Wu, K. C., Welding of Aluminum-Boron Composites, Proc. 5th Nat. SAMPE Tech. Conf. (Oct. 1973).
7. Lehman, G. M., Fundamentals of Joint Design for Composite Airframes, Douglas Paper 5263, WESTEC Conf. (Mar. 1969).
8. Hersh, M. S. and Featherby, M., Joining of Boron/Aluminum Composites, AIAA Paper No. 72-360 (Apr. 1972).
9. Mitchell, R. A., Woolley, R. M., and Chwirut, D. J., Composite-Overlay Reinforcement of Cutouts and Cracks in Metal Sheet, NBSIR 73-201 (Feb. 1973).
10. Mitchell, R. A., Woolley, R. M., and Chwirut, D. J., Analysis of Composite-Reinforced Cutouts and Cracks, J. AIAA (June 1975).
11. Zienkiewicz, O. C., The Finite Element Method in Engineering Science, McGraw-Hill (1971).
12. Wilson, E. L., Finite Element Analysis of Two-Dimensional Structures, Structures and Materials Research Report No. 63-2, U. of Calif. Berkeley (June 1963).

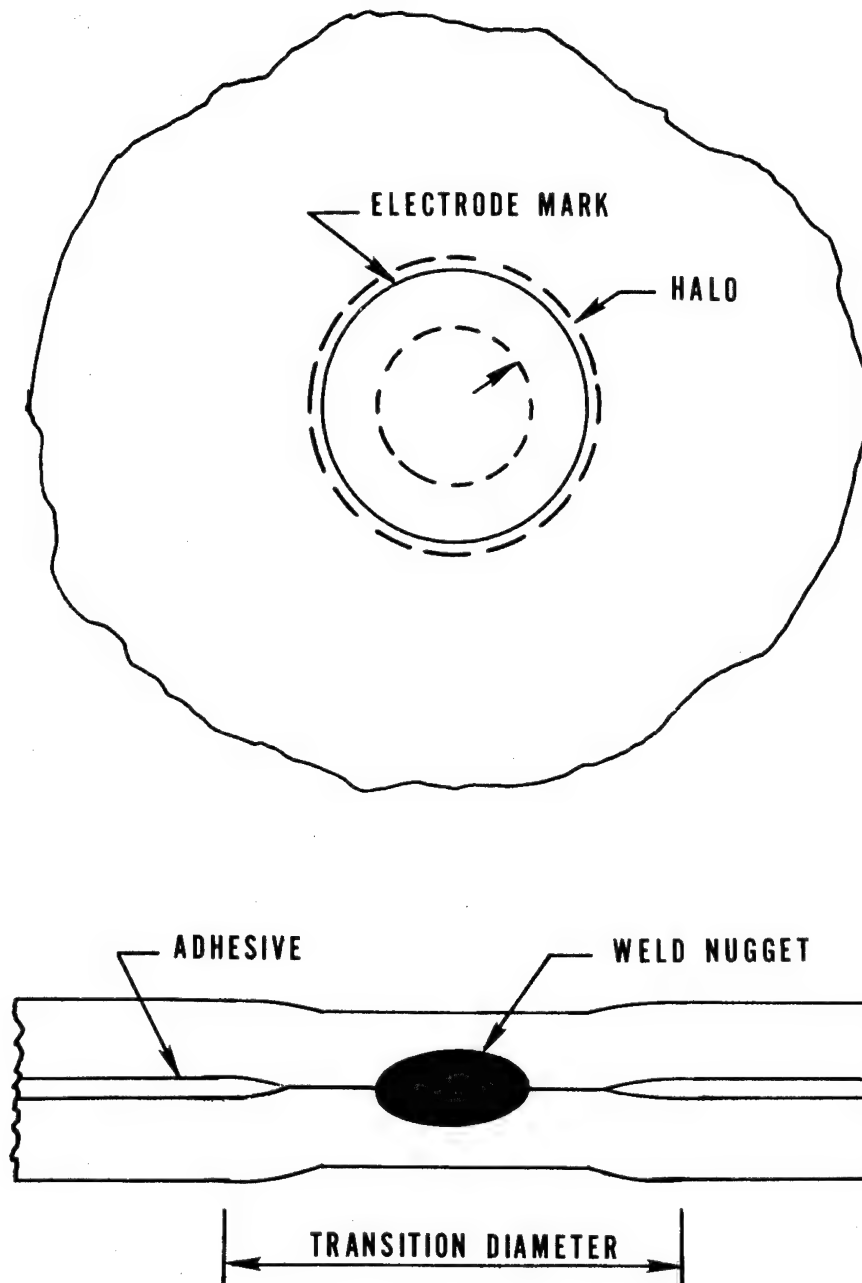


FIGURE 1. SCHEMATIC DESCRIPTION OF A SPOTWELD IN A SINGLE-LAP WELDBONDED JOINT.

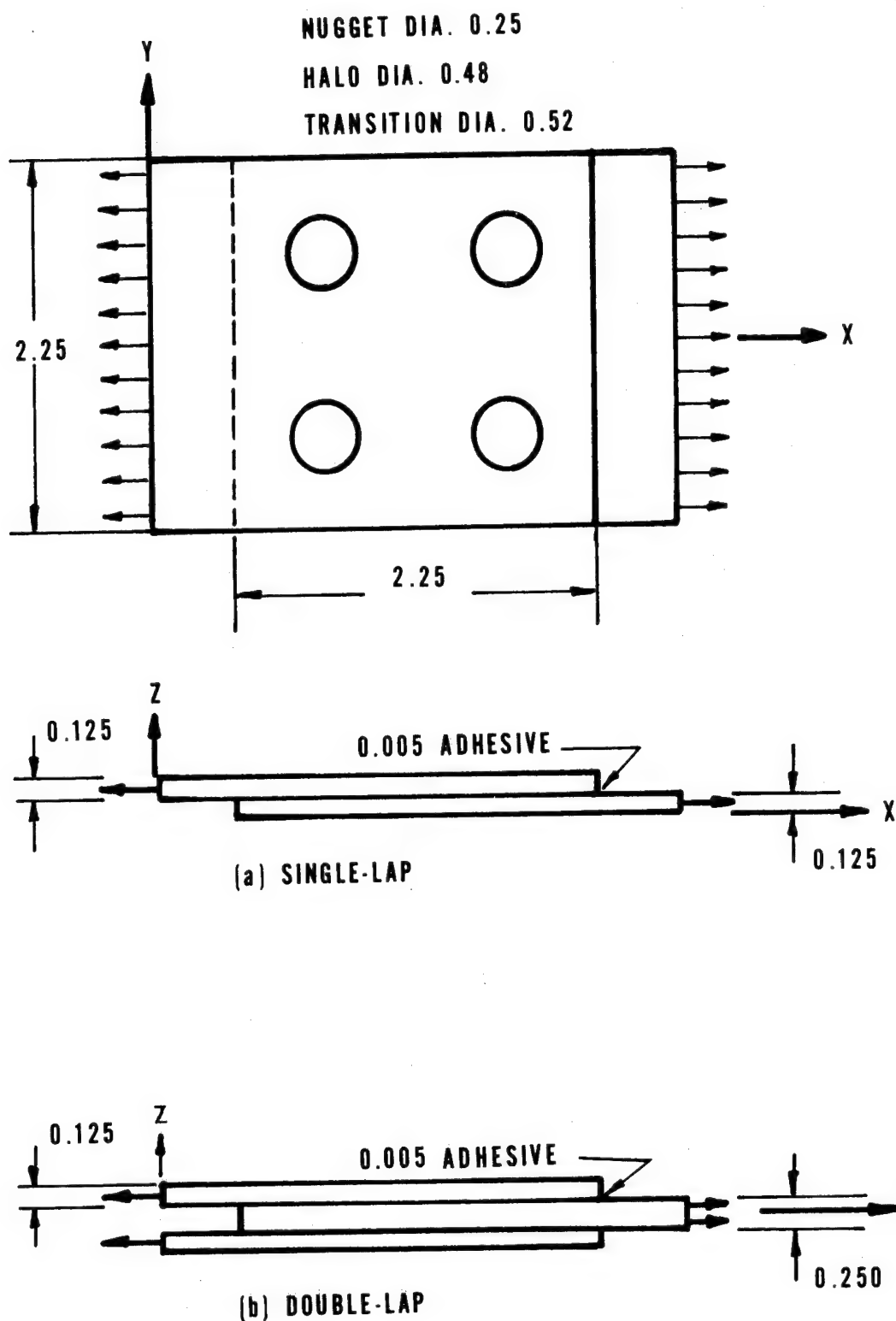
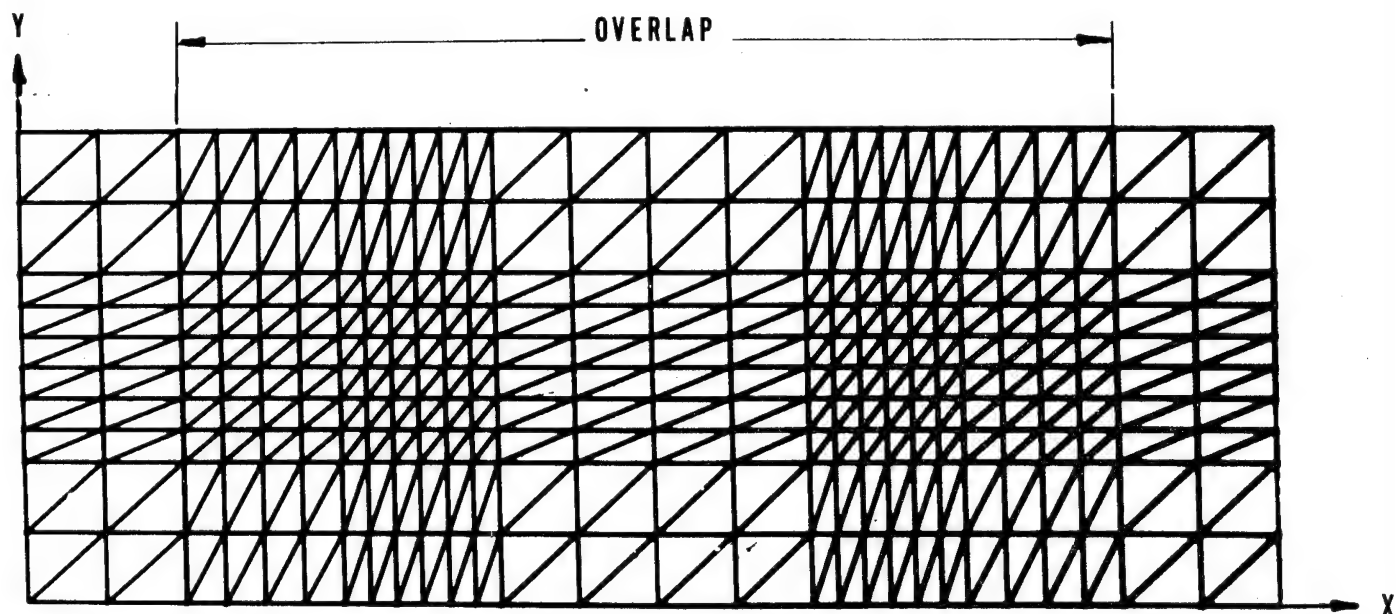
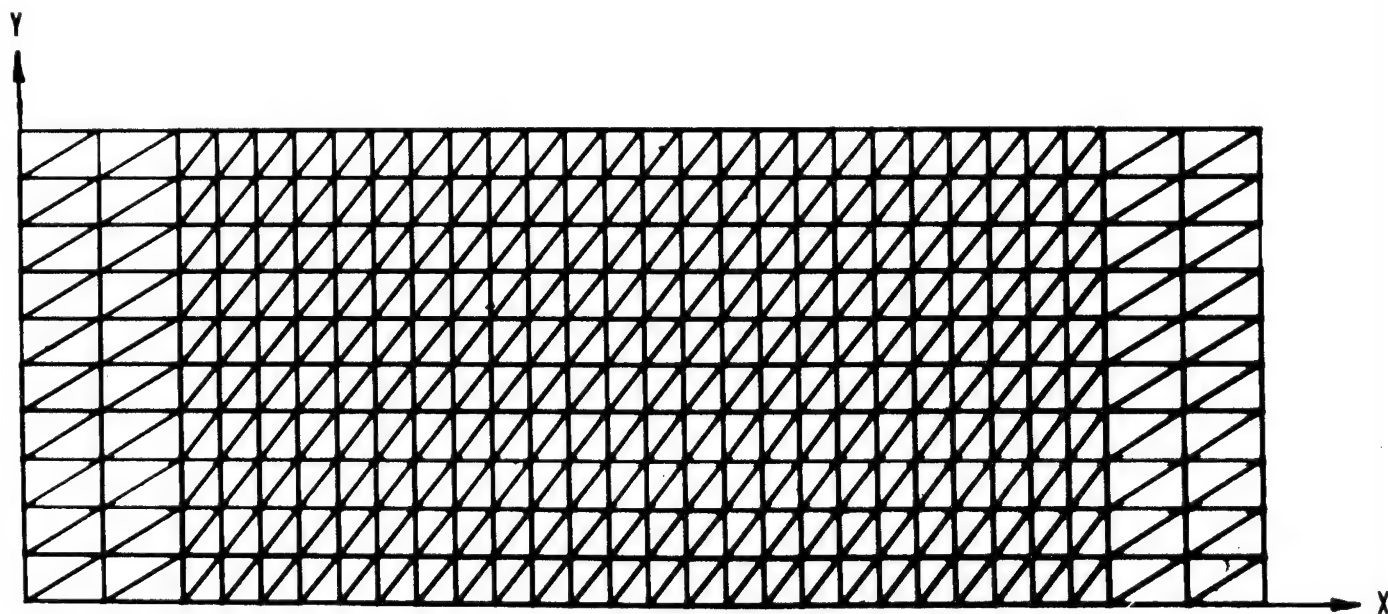


FIGURE 2. COMPARABLE SINGLE-LAP AND DOUBLE-LAP WELDBONDED JOINTS. DIMENSIONS ARE IN INCHES (1 in = 2.54 cm).

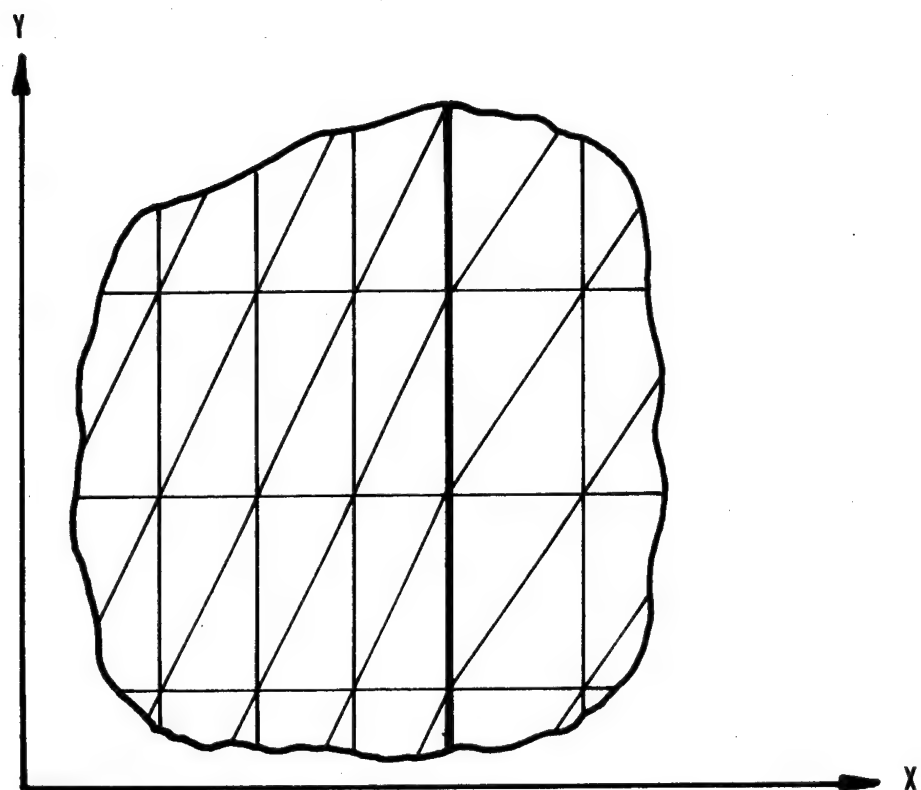


(a) WELDBONDED AND SPOTWELDED

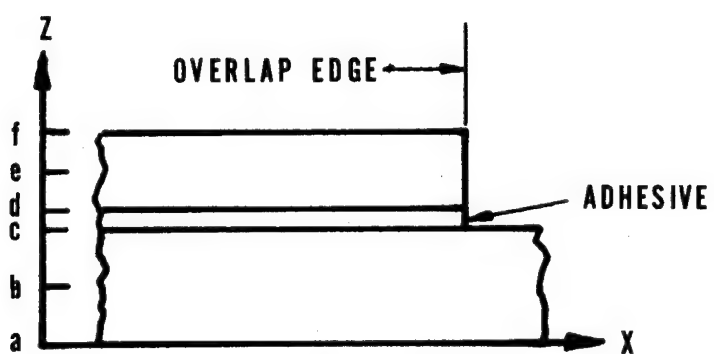


(b) BONDED

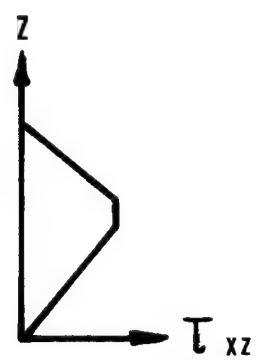
FIGURE 3. FINITE ELEMENT MESHES USED FOR PLANFORM ANALYSIS OF A WELDBONDED JOINT, A SPOTWELDED JOINT, AND A BONDED JOINT.



(a) TRIANGULAR ELEMENT NETWORK (PLAN)

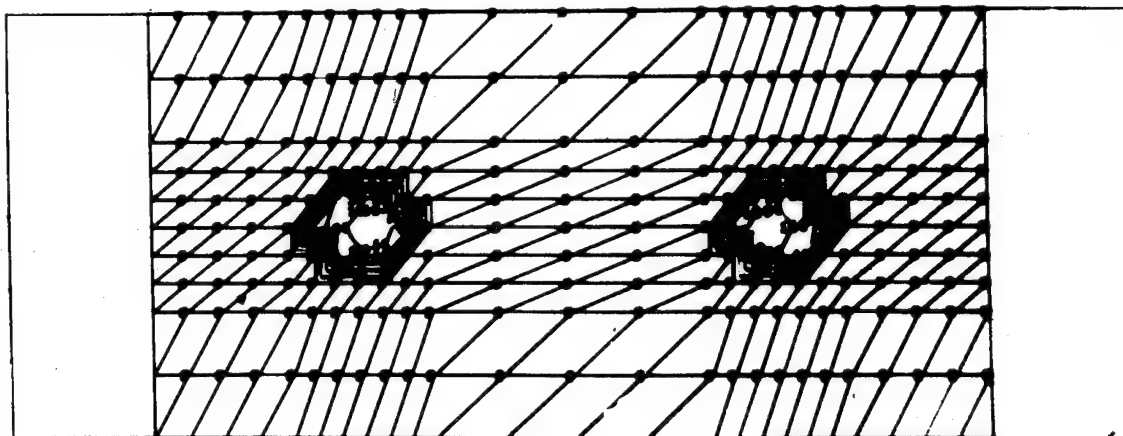


(b) CROSS SECTION

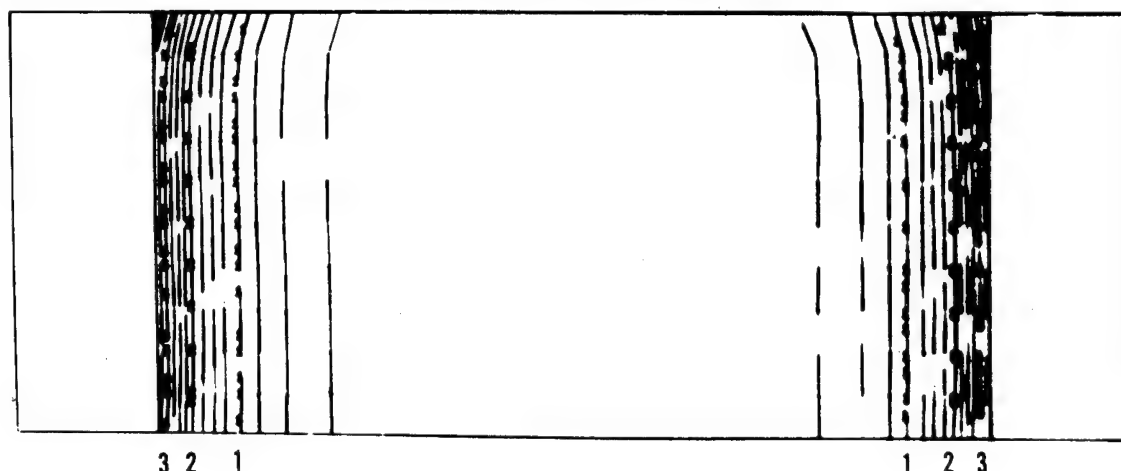


(c) SHEAR STRESS
(ASSUMED)

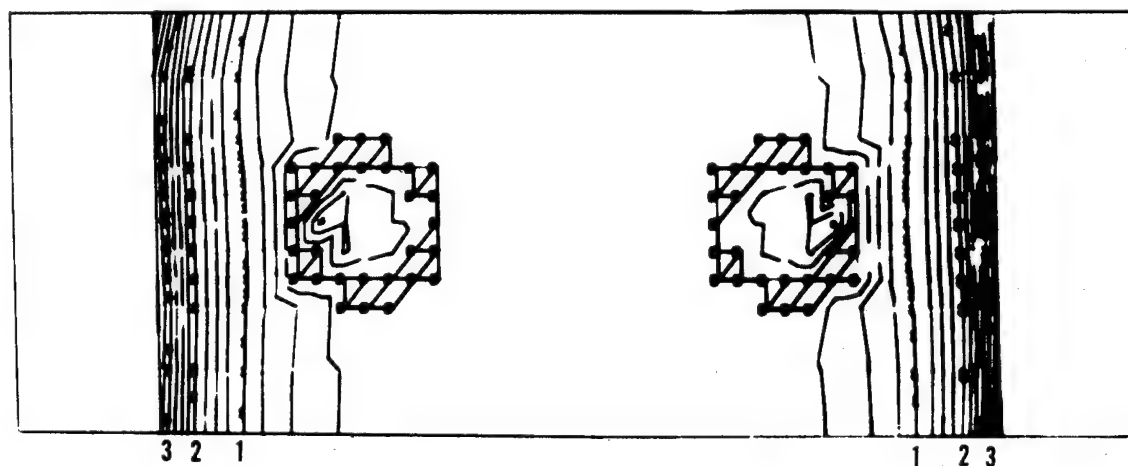
FIGURE 4. SCHEMATIC BASIS FOR SHEAR-STIFFNESS ELEMENT.



(a) SPOTWELDED
CONTOUR INTERVAL 4000 LABEL INTERVAL 8000



(b) BONDED
CONTOUR INTERVAL 250 LABEL INTERVAL 1000



(c) WELDBONDED
CONTOUR INTERVAL 250 LABEL INTERVAL 1000

FIGURE 5. CONTOUR PLOTS OF RESULTANT LAP SHEAR STRESS IN SINGLE-LAP JOINTS.

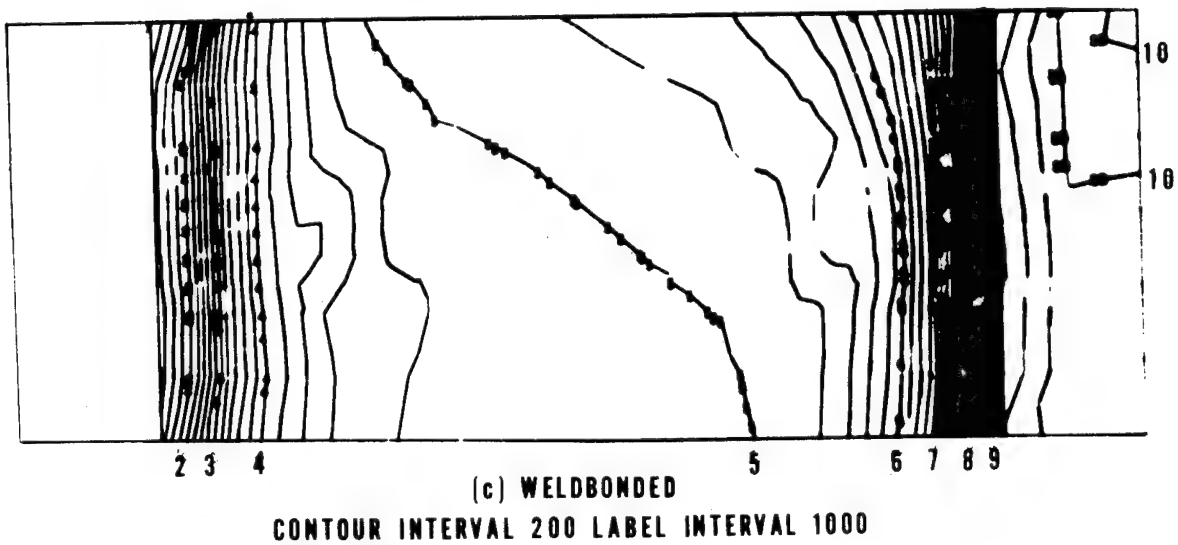
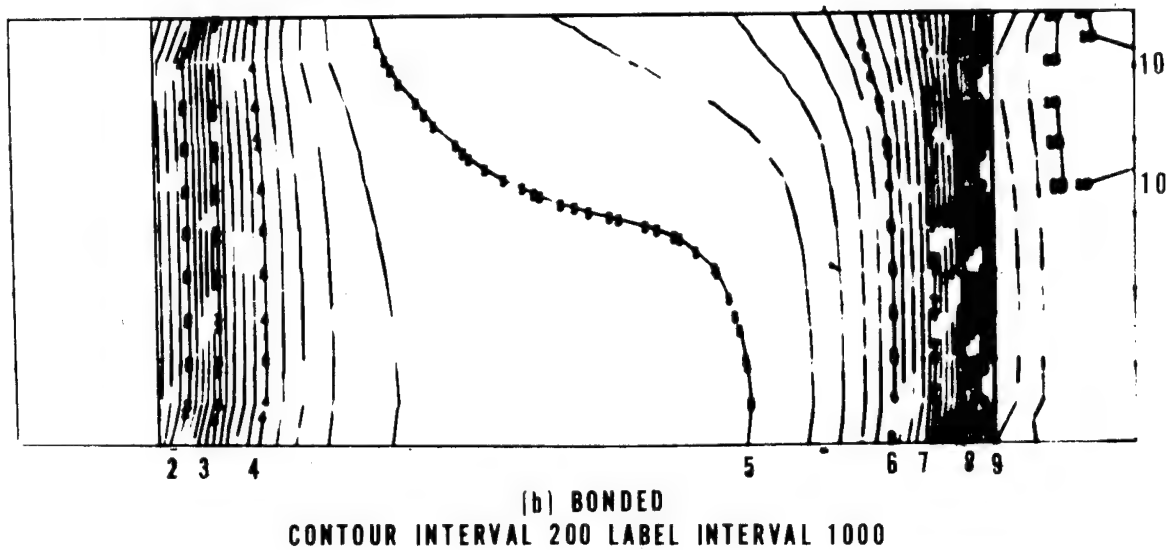
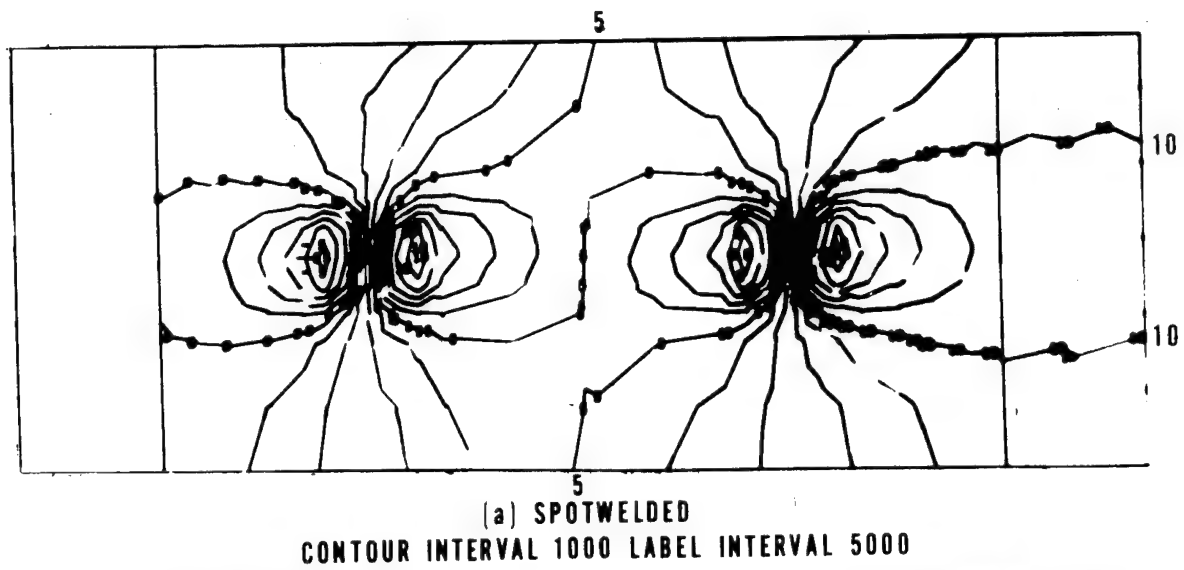
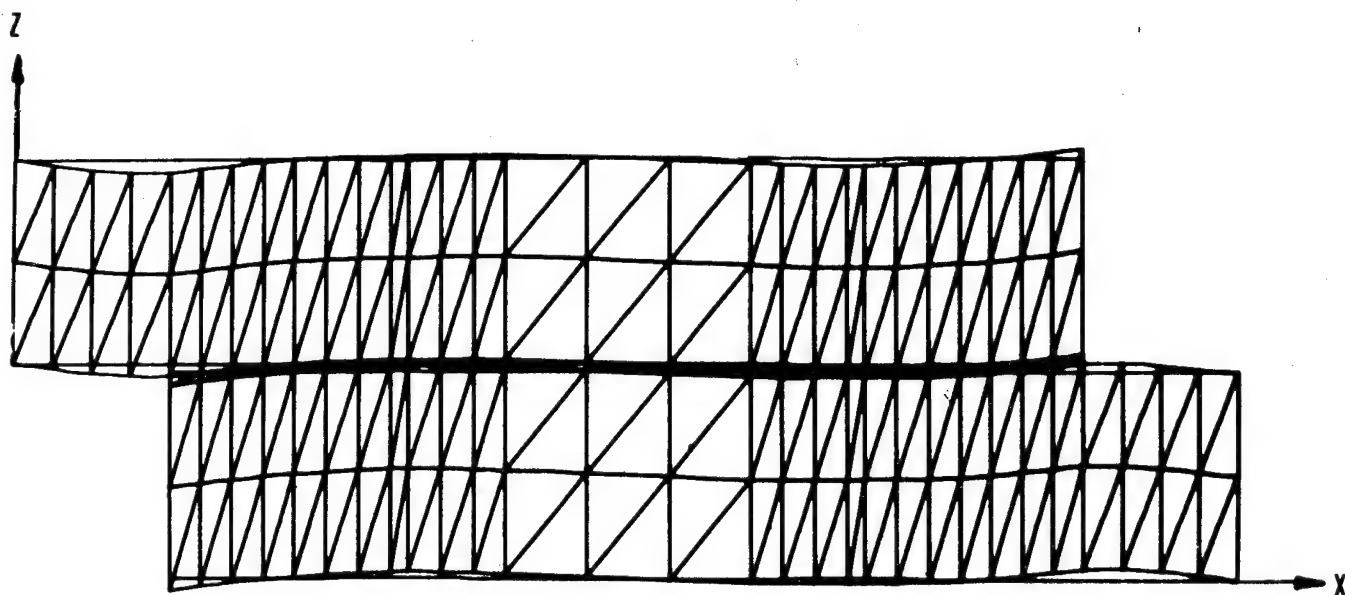
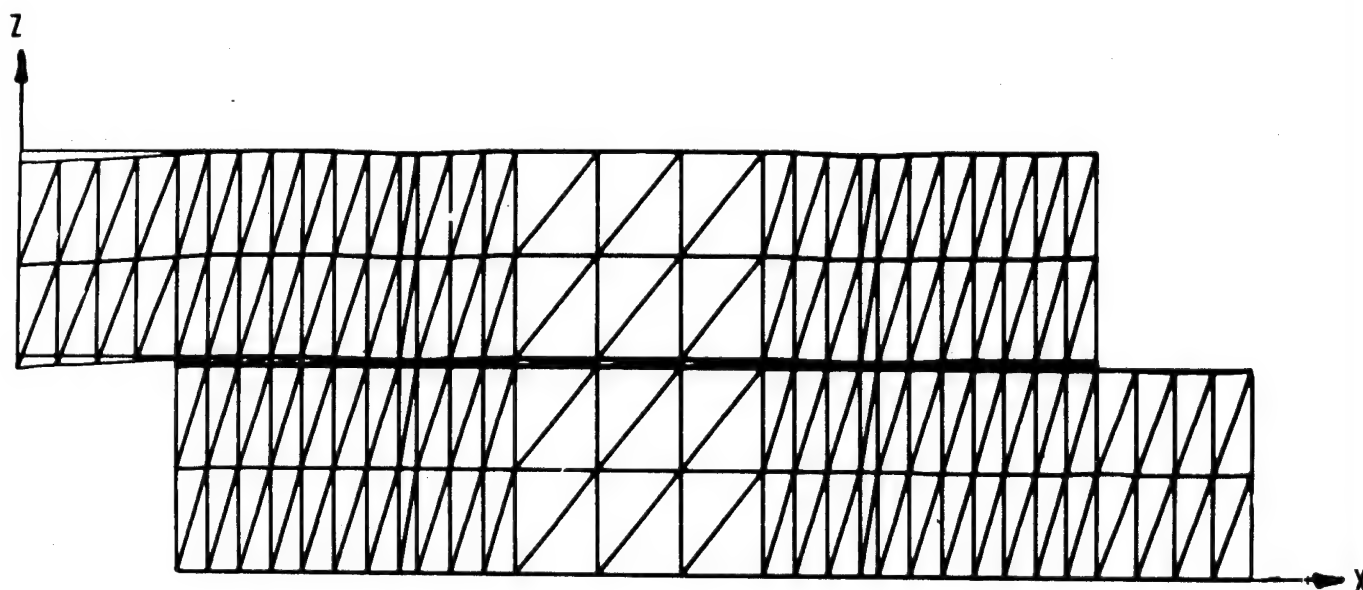


FIGURE 6. CONTOUR PLOTS OF THE X COMPONENT OF NORMAL STRESS IN THE RIGHTMOST SHEETS OF SINGLE-LAP JOINTS.

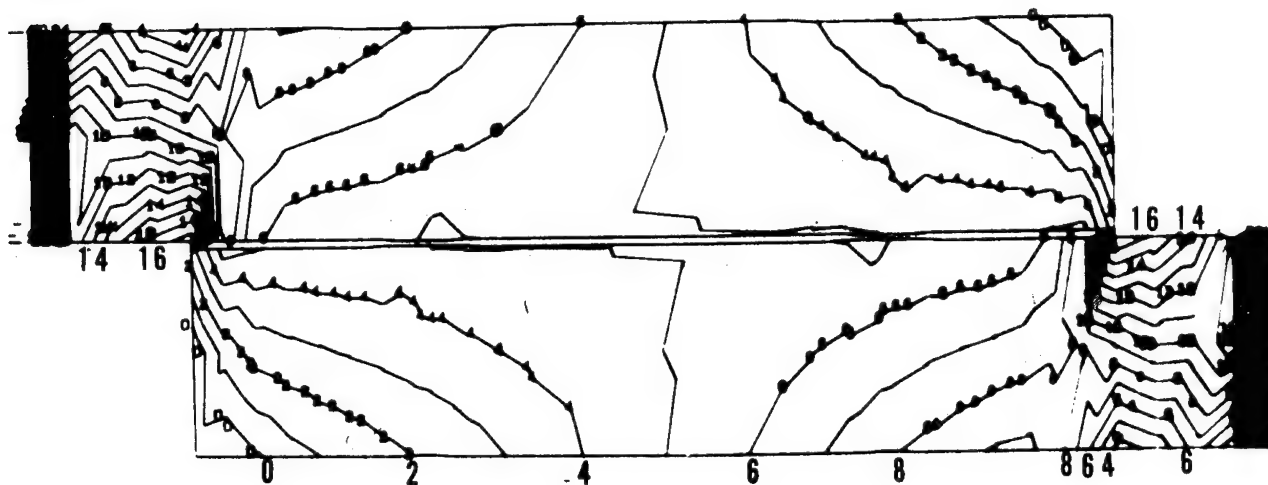


(a) SINGLE-LAP

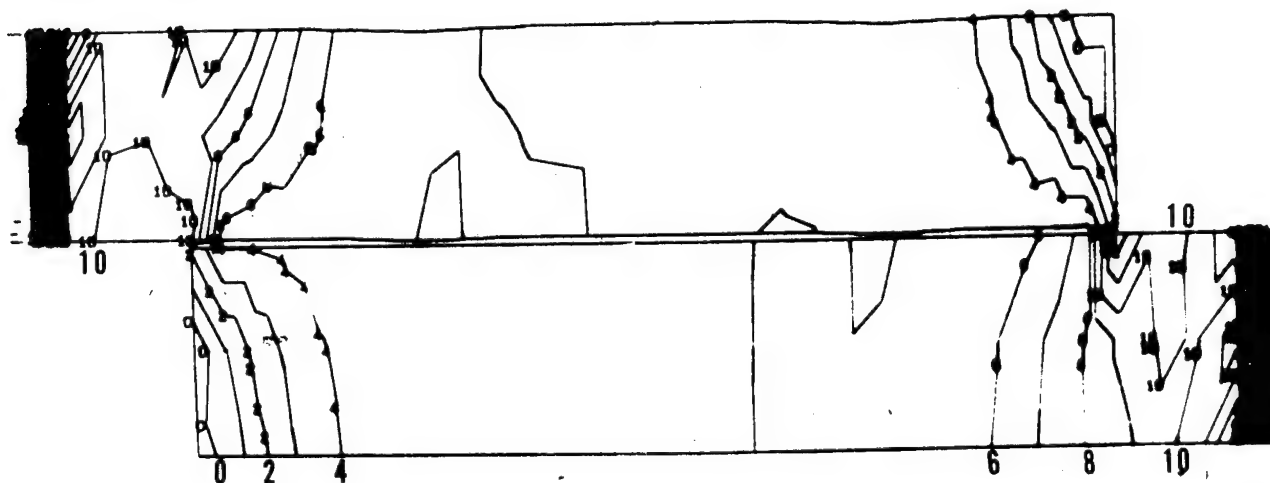


(b) DOUBLE-LAP

FIGURE 7. FINITE ELEMENT MESHES USED FOR LONGITUDINAL CROSS-SECTION ANALYSIS OF COMPARABLE SINGLE-LAP AND DOUBLE-LAP WELDBONDED JOINTS. THICKNESS DIMENSIONS EXAGGERATED 4 TIMES, VERTICAL DEFLECTIONS EXAGGERATED 20 TIMES.



(a) SINGLE-LAP
CONTOUR INTERVAL 1000 LABEL INTERVAL 2000



(b) DOUBLE-LAP
CONTOUR INTERVAL 1000 LABEL INTERVAL 2000

FIGURE 8. CONTOUR PLOTS OF THE X COMPONENT OF NORMAL STRESS IN COMPARABLE SINGLE-LAP AND DOUBLE-LAP WELDBONDED JOINTS.

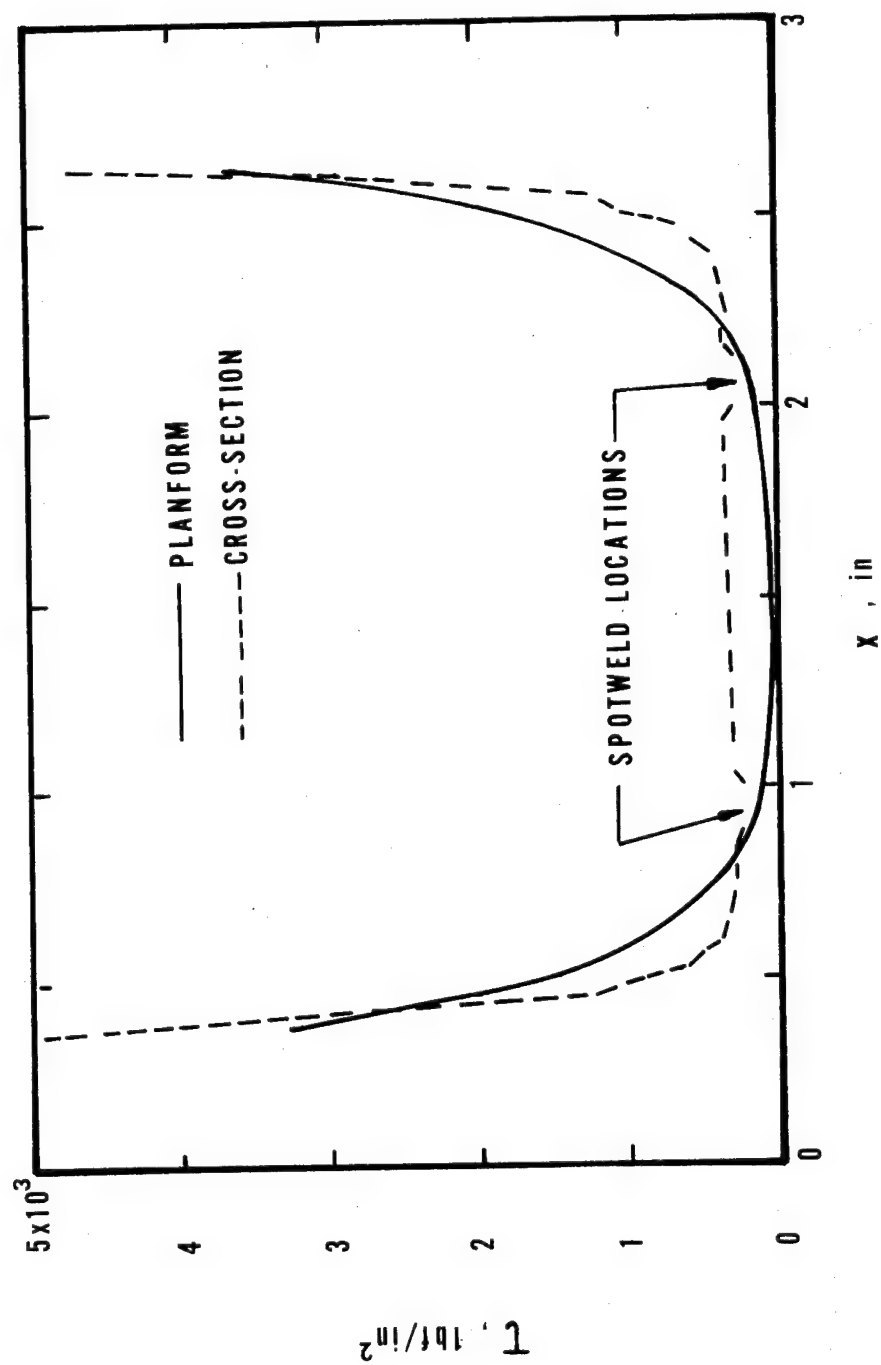


FIGURE 9. ADHESIVE LAP SHEAR STRESS IN SINGLE-LAP WELDBONDED JOINT, FROM PLATFORM ANALYSIS AND CROSS-SECTION ANALYSIS.

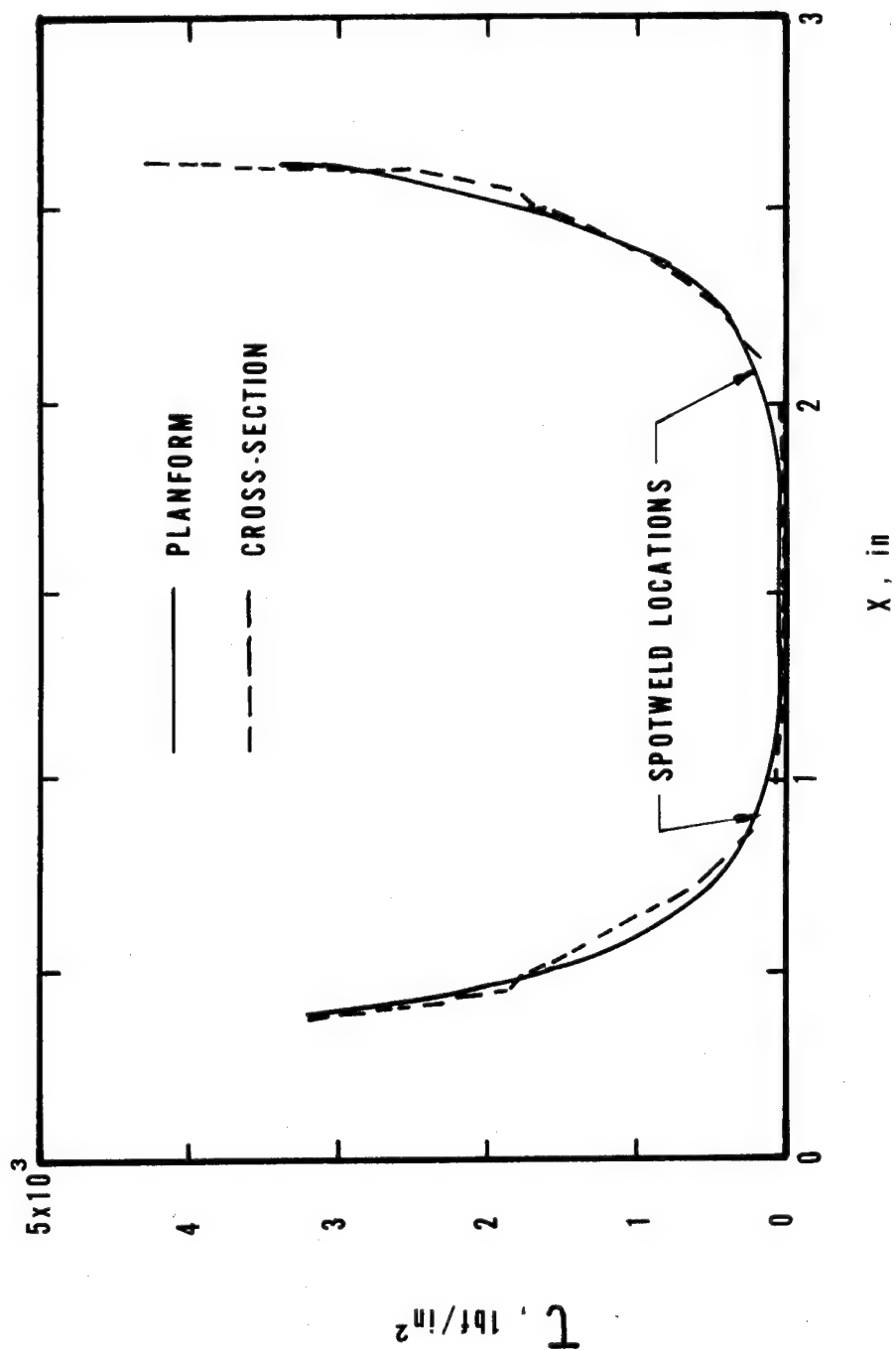


FIGURE 10. ADHESIVE LAP SHEAR STRESS IN DOUBLE-LAP WELDBONDED JOINT, FROM PLANFORM ANALYSIS AND CROSS-SECTION ANALYSIS.

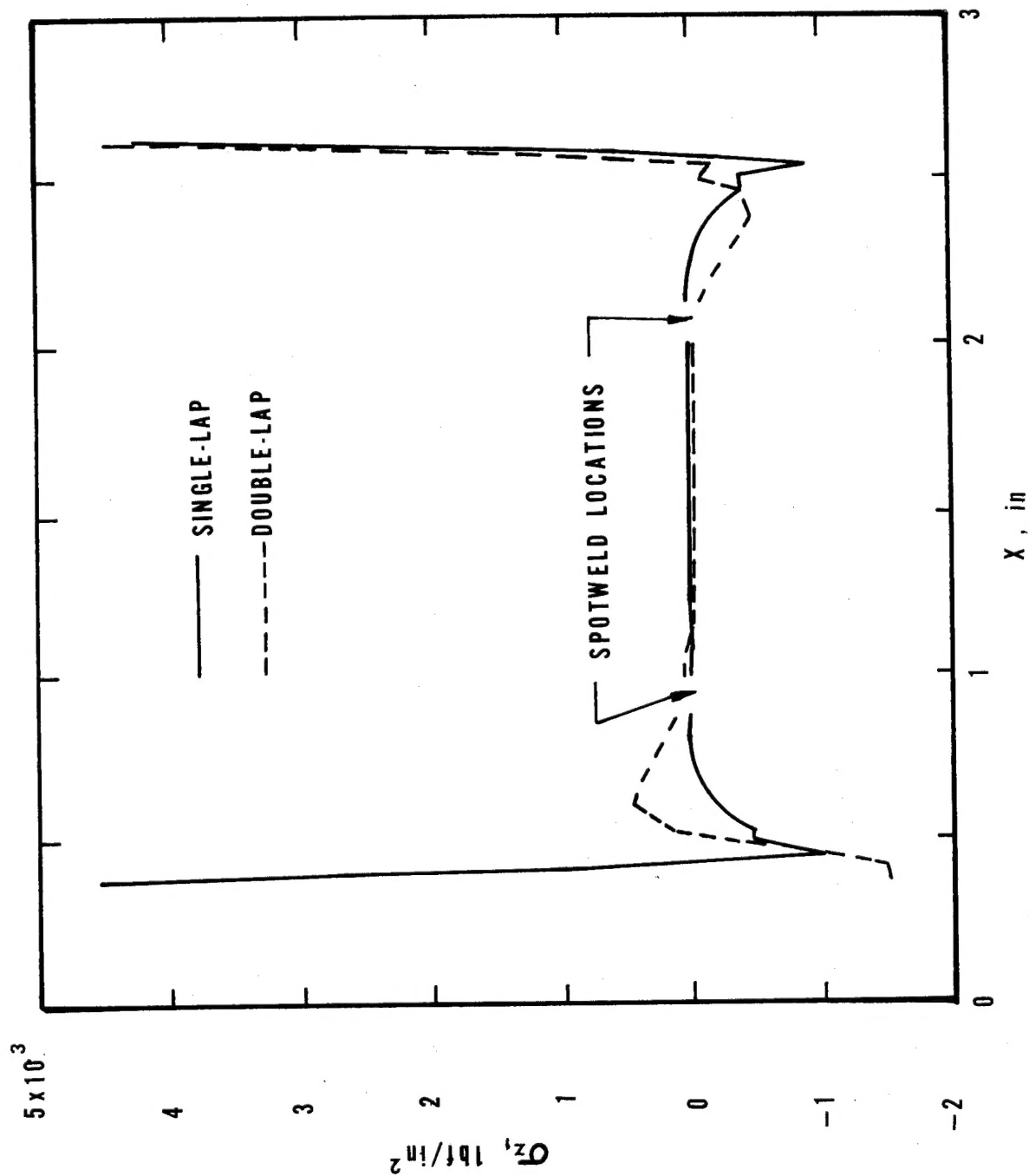


FIGURE 11. ADHESIVE NORMAL STRESS (PEEL COMPONENT) IN COMPARABLE SINGLE-LAP AND DOUBLE-LAP WELDBONDED JOINTS, FROM CROSS-SECTION ANALYSIS.

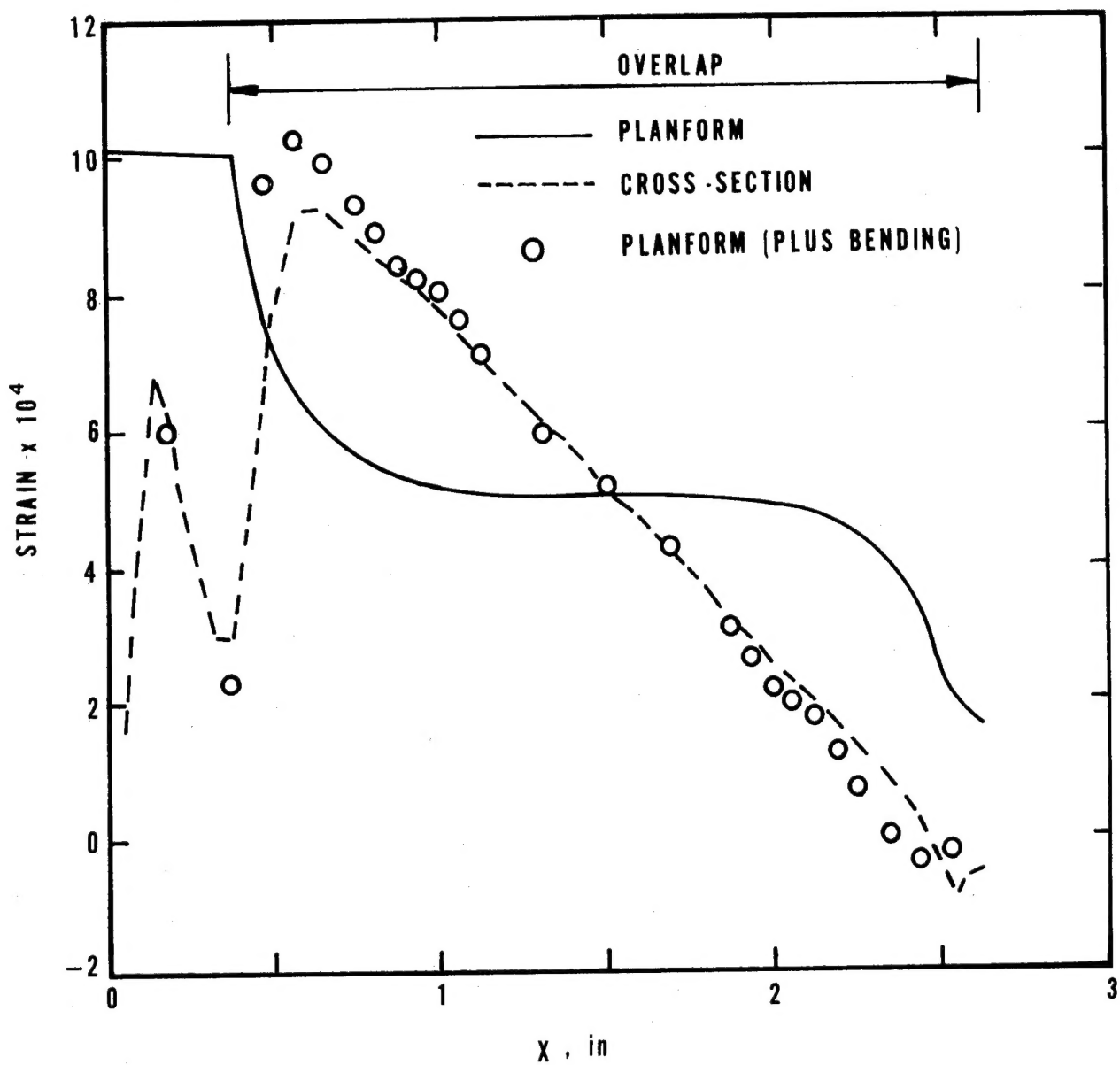


FIGURE 12. LONGITUDINAL STRAIN ON SURFACE OF SINGLE-LAP WELDBONDED JOINT.

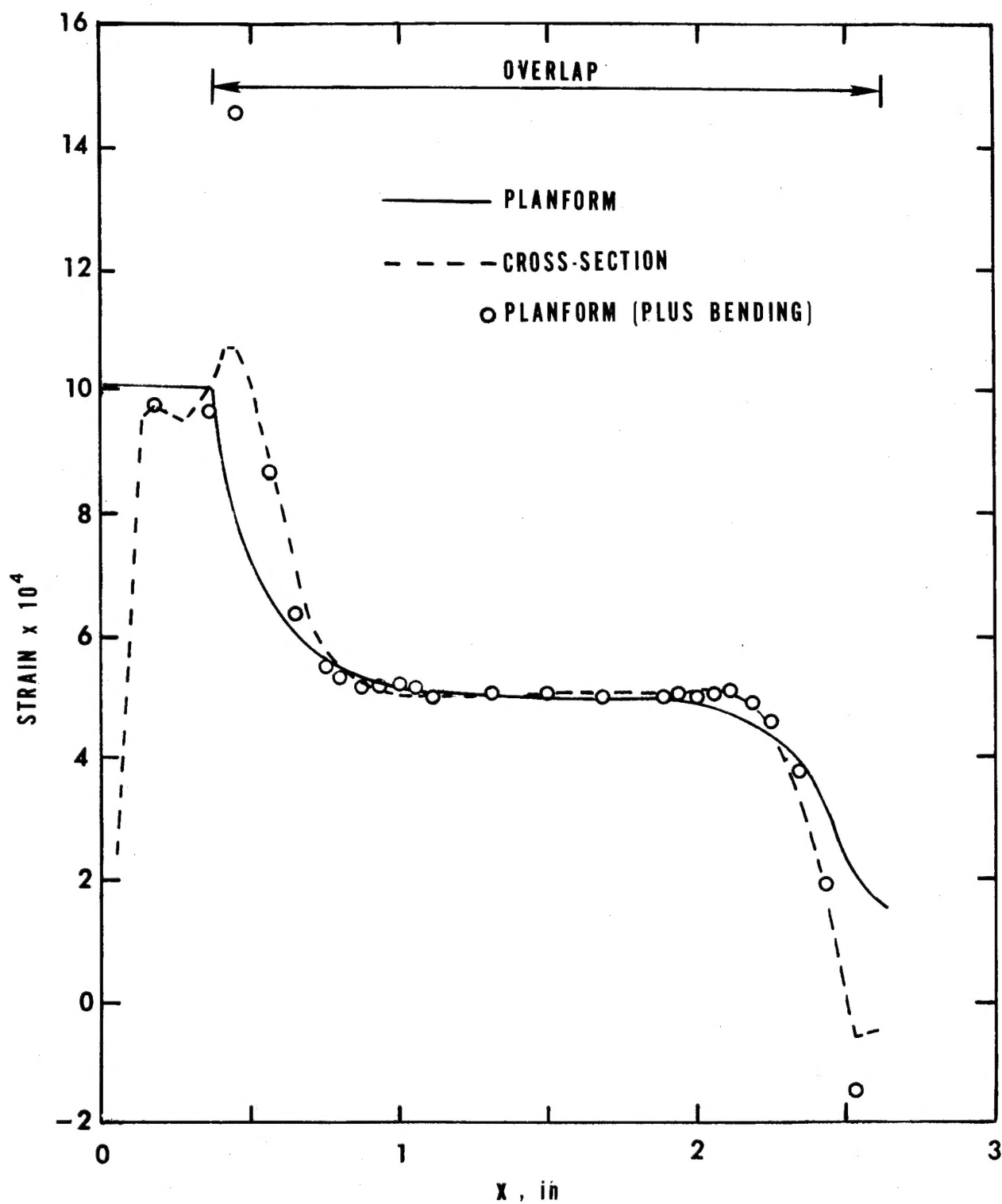


FIGURE 13. LONGITUDINAL STRAIN ON SURFACE OF DOUBLE-LAP WELDBONDED JOINT.

U.S. DEPT. OF COMM. BIBLIOGRAPHIC DATA SHEET	1. PUBLICATION OR REPORT NO. NBSIR 75-957	2. Gov't Accession No.	3. Recipient's Accession No.
4. TITLE AND SUBTITLE FINITE ELEMENT ANALYSIS OF SPOTWELDED, BONDED AND WELDBONDED LAP JOINTS		5. Publication Date December 1975	
		6. Performing Organization Code	
7. AUTHOR(S) Richard A. Mitchell, Ruth M. Woolley, and Saul M. Baker		8. Performing Organ. Report No.	
9. PERFORMING ORGANIZATION NAME AND ADDRESS NATIONAL BUREAU OF STANDARDS DEPARTMENT OF COMMERCE WASHINGTON, D.C. 20234		10. Project/Task/Work Unit No. 2130141	
		11. Contract/Grant No.	
12. Sponsoring Organization Name and Complete Address (Street, City, State, ZIP) National Bureau of Standards Department of Commerce Washington, D. C. 20234		13. Type of Report & Period Covered Final Report	
		14. Sponsoring Agency Code	
15. SUPPLEMENTARY NOTES			
16. ABSTRACT (A 200-word or less factual summary of most significant information. If document includes a significant bibliography or literature survey, mention it here.) Finite element computer analyses of single-lap and double-lap structural joints are described. A planform analysis articulates the in-plane deformation of the joined sheet material and the lap-shear stresses acting through the spotwelds and/or adhesive. A longitudinal cross-section analysis computes out-of-plane bending effects, particularly important in single-lap joints, and adhesive peel stresses. Numerical results are presented that suggest a reasonable degree of mutual consistency between the planform analysis and the cross-section analysis. Although the basic finite element formulation is linear, nonlinear deformation can be simulated by a series of linear solutions. The computer output includes contour plots of stress and strain fields and exaggerated-scale plots of displacements.			
17. KEY WORDS (six to twelve entries; alphabetical order; capitalize only the first letter of the first key word unless a proper name; separated by semicolons) Adhesive-bonded joints; bonded joints; double-lap joint analysis; finite element analysis; joining; joints; single-lap joint analysis, single-lap-joint bending; spotwelded joints; weldbonded joints.			
18. AVAILABILITY <input checked="" type="checkbox"/> Unlimited <input type="checkbox"/> For Official Distribution. Do Not Release to NTIS <input type="checkbox"/> Order From Sup. of Doc., U.S. Government Printing Office Washington, D.C. 20402, SD Cat. No. C13 <input checked="" type="checkbox"/> Order From National Technical Information Service (NTIS) Springfield, Virginia 22151		19. SECURITY CLASS (THIS REPORT) UNCLASSIFIED	21. NO. OF PAGES 24
		20. SECURITY CLASS (THIS PAGE) UNCLASSIFIED	22. Price \$3.50